Chen *et al.*
Journal of Engineering and Applied Science (2022) 69:94
https://doi.org/10.1186/s44147-022-00131-2

Journal of Engineering and Applied Science

RESEARCH Open Access

Failure analysis of weld cracking of gas gathering pipeline in dewatering station

Yong Chen[1,2*], Yi Xie[1], Wenjing Wang[3] and Jichuan Li[4]

*Correspondence:
chyswpu@163.com

[1] School of Mechatronic Engineering, Southwest Petroleum University, Chengdu 610500, Sichuan, China
[2] Oil and gas equipment technology Sharing and Service Platform of Sichuan Province, Chengdu, China
[3] Sichuan Changning Natural Gas Development Co., Ltd. of PetroChina Southwest Oil and Gas Field Company, Chengdu, China
[4] Institute of Safety, Environmental Protection and Technical Supervision, PetroChina Southwest Oil & Gasfield Company, Chengdu, Sichuan, China

Abstract

There are a lot of welded joints in the shale gas collection pipeline, so the failure risk of the shale gas production line is very high. A leak has occurred in the gas collection pipeline of a dewatering station, and in order to find out the causes of failure and provide technical support for safe shale gas transmission, macroscopic analysis, non-destructive testing (X-ray flaw detection), mechanical properties, and metallurgical analysis were performed on the failed pipe section, and CFD method was used to further analyze the failure mechanism of the ring weld pipe. The macroscopic analysis yielded the weld height is significantly greater than the standard minimum requirement. Non-destructive testing showed a large number of cracks with varying degrees of extension along the weld circumference on the inner surface of the weld. The chemical composition and mechanical properties of the pipe and the weld met the requirements. The microstructure of the base metal met the standard. There are no inclusions, holes, unfused areas, or other welding defects in the weld zone. The cracks originate from the weld fusion zone, and there are a large number of intergranular microcracks. CFD simulation results show that although the stress concentration caused by the height of the weld does not directly lead to weld cracking, under the influence of the stress concentration, cracks tend to sprout at the coarse grain organization of the fusion zone on the inner surface of the weld and can easily propagate throughout the weld and pipe wall thickness, leading to crack damage. Several suggestions to prevent such a failure were proposed to avoid the occurrence of similar accidents.

Keywords: Gas gathering pipelines, Weld, Failure analysis, CFD simulation

Introduction

The breakthrough of shale gas mining technology has brought about a surge in shale gas production. As a result, the installation of gas gathering pipelines is increasing, and there will be a large number of welded joints in gas gathering pipelines. Each welded joint is composed of the base metal, the weld metal, and the heat-affected zone. The mechanical properties of each part are different. Therefore, the butt weld area is prone to failure relative to the entire pipe [1–8]. A gas gathering pipeline of a dewatering station had a leak 2 months after it was put into operation. After investigation and excavation, it was found that cracks appeared in the heat-affected area of the weld of the pipeline. In the process of shale gas production, the pipeline welds have repeatedly failed, which has caused huge economic losses to the production. It is urgent to conduct in-depth analysis

on the failure causes of the gas gathering pipeline, so as to provide technical support and reference for the safe application of pipelines.

Gen et al. [9] conducted a comprehensive analysis on the fracture failure of a circumferential weld of a gas gathering pipeline containing H2S and concluded that sulfide stress cracking of a circumferential weld may be the main cause of fracture failure. Jun et al. [10] studied the failure events of girth weld in a natural gas station and considered that the reason causing welding defects of girth weld is that the slag inclusions were not cleaned up timely, and then, the slag inclusions led to the existence of welding defects. Qiang et al. [11] studied the cracking failure of a boiling gas (BOG) pressurized pipeline weld in liquefied natural gas (LNG) receiving station and studied the influence of compressor vibration on welding by finite element simulation analysis method. The experimental results show that a large number of inclusions and super-size second phase are produced in the weld, and microcracks appear around the inclusions and the second phase. The finite element analysis (FEA) calculation results show that the vibration of the compressor does not directly lead to weld cracking. However, under the influence of vibration, multi-source solidification cracks and micro-cracks originate from the butt weld surface and propagate to the entire weld, which is the reason for crack failure. Shabani et al. [12] analyzed the failure of 30-in diameter gas pipeline and studied the mechanism and morphology of crack initiation and propagation. The results show that the failure reason is the longitudinal crack on the longitudinal weld centerline, and some factors related to sulfide stress cracking (SSC) and metallurgical defects lead to the failure of welded joint. Zhao et al. [13] analyzed the gas explosion pipeline. The results show that the stress corrosion cracking (SCC) in the pipeline mechanical damage zone is the cause of failure. Qiao et al. [14] studied the corrosion damage at a weld joint based on the heterogeneity of natural gas gathering pipeline. The results show that the geometric discontinuity of the welded joint is the main cause of accelerated corrosion damage at the joint. The change of the wall thickness of the welded pipe not only produces a gas eddy, but also leads to stress concentration. Lixia et al. [15] studied the internal and external causes of the failure of a girth weld. It is considered that the collapse of the slope along the pipeline and the settlement of the ground aggravate the stress concentration at the root welding defect, which is the external cause of the leakage failure of the girth weld. Yuguang et al. [16] studied the fracture mechanism and behavior of a pipeline girth weld. The results show that due to the softening of the material in the heat affected zone, the crack initiates at the interface between the weld line on the inner wall of the pipeline and the heat affected zone, and then, the crack expands outward from the inner wall until a penetrating crack is formed. Finally, the crack propagates rapidly along the circumferential direction, resulting in the overall failure of the pipeline. Xu et al. [17] studied fatigue properties for the weld joint of the X80 weld pipe before and after removing the weld reinforcement and think that the fatigue crack always initiates at the inner weld toe. Zhang et al. [18] studied effect of stress concentration on the fatigue strength of A7N01S-T5 welded joints. The results show that the butt joints with the weld reinforcement have much lower fatigue strength than joints without the weld reinforcement, stress concentration is a key factor that affects the fatigue strength of welded joints, and stress concentration introduced by the weld reinforcement should be controlled.

In the present case, in order to find out the reasons for the failure, the failed part of the pipeline was intercepted and checked through macroanalysis, non-destructive testing (X-ray flaw detection), mechanical properties, and metallographic analysis. CFD simulation was used to further analyze the stress concentration effect of the pipe. Finally, the causes of failure are summarized, and countermeasures to avoid similar failures are proposed.

Methods

The focus of this paper is the failure analysis of the weld, and this study evolved through a series of steps which are as follows:

1) Firstly, a macroscopic analysis is performed to determine whether the dimensions, wall thickness, and the height of the weld meet the standard requirements, and then, a nondestructive inspection is performed to determine the crack distribution.
2) Secondly, after mechanical properties and metallurgical analysis of the base material as well as the weld to determine whether the pipe base material properties meet the standards and whether there are welding defects in the weld.
3) Then, the finite element model is established and the boundary conditions are set according to the actual dimensions.
4) Finally, the causes of failure are summarized, and relevant suggestions and measures are proposed.

Experimental analysis

Macroanalysis

External inspection and measurement of the pipe showed no obvious signs of corrosion pits inside or outside the pipe (Fig. 1). In the direction of 12 o'clock position, on the outer surface of the pipe near the side of the B pipe section, there is a crack that extends along the circumference of the weld with a crack length of about 40 mm and corresponds to the presence of a circumferential crack of about 140 mm in length and 0.46 mm in width on the inner surface of the weld. As shown in Fig. 2.

The measured wall thickness of the pipe meets the minimum required wall thickness of 6.3mm, and there is no significant difference between the wall thickness of A and B pipe sections, where the average wall thickness of A pipe section is 7.02mm and the average wall thickness of B pipe section is 6.96mm. Dimensional measurement results are shown in Table 1. The root welding height, the cover welding height, and the misalignment of the weld were checked, and the results are shown in Table 2. The maximum and average values of the root welding height are 4.6mm and 3.03mm,

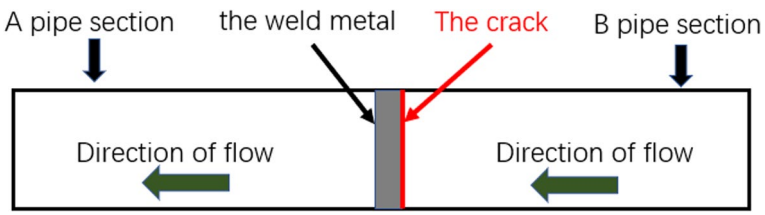

Fig. 1 Schematic diagram of A and B pipe sections

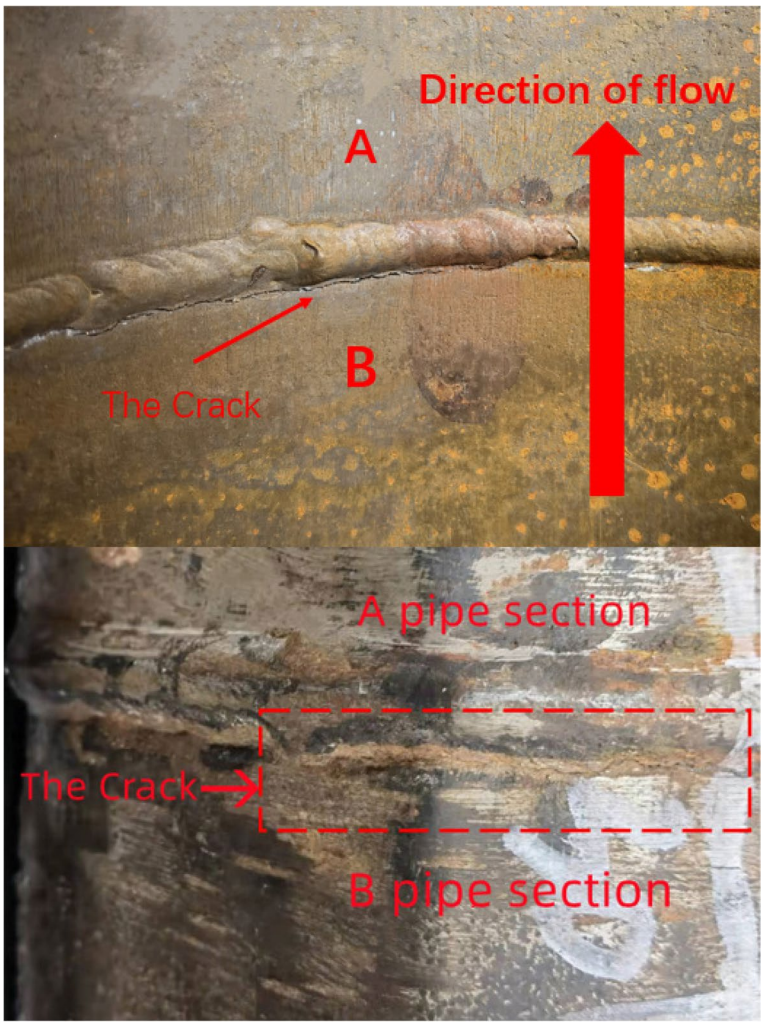

Fig. 2 Macroscopic appearance of pipeline weld position

Table 1 The wall thickness measurement results (mm)

Measurement category	1	2	3	4	mean value
A pipe section	7.06	7.12	7.04	6.84	7.02
B pipe section	6.95	7.02	6.96	6.91	6.96

Table 2 Weld quality inspection (mm)

Specimen number	1#	2#	3#	4#	Mean value
Measurement category	12 o'clock direction (crack location)	9 o'clock direction	6 o'clock direction	3 o'clock direction	
The root welding height	4.6	3.5	2.1	1.9	3.03
The cover welding height	2.5	1.7	1.6	2.3	2.025

Table 3 Length of weld crack

Numbering	Crack length (mm)
1#	90
2#	120
3#	40
4#	10
5#	5
6#	132

Table 4 Chemical constituents of pipe materials (Wt%)

Numbering element	Maximum content (wt%)		
	A pipe section	B pipe section	GB/T9711-2017 standard requires
C	0.134	0.13	≤0.24
Si	0.25	0.255	≤0.45
Mn	1.363	1.327	≤1.4
P	0.011	0.015	≤0.025
S	0.003	0.004	≤0.015
Cr	0.071	0.062	≤0.3
Mo	0.013	0.01	≤0.15
Ni	0.032	0.032	≤0.3
Nb	0.025	0.037	≤ 0.05
V	0.075	0.062	≤ 0.1
Ti	0.002	0.015	≤ 0.04
Cu	0.032	0.044	≤0.5
B	<0.0001	<0.0001	≤0.001
V+Ti+Nb	0.102	0.054	≤0.15
Carbon equivalent (CE_{IIW})	0.397	0.383	≤0.43

Table 5 Results of tensile test

Item/test specimen	Specimen size (width × gauge)	Tensile strength (MPa)	Yield strength (MPa)	Yield strength ratio	Elongation (%)
1	15×50mm	527	392	0.74	32
2		531	395	0.74	31
3		533	397	0.74	30
Mean value		530	395	0.74	31
GB/T9711-2017		460~760	360~530	≤0.93	≥20

respectively; the average value of the cover weld height is 2.025mm and there is a misalignment of the weld; and the maximum misalignment is 0.4mm.

The execution standard of steel pipe welding is "GB/T31032-2014 Welding and acceptance standard for steel pipings and pipelines". Weld quality control standards

Table 6 Results of tensile test

Item/test specimen	Specimen size (width × gauge)	Tensile strength (MPa)	Yield strength (MPa)	Yield strength ratio	Elongation (%)
1	12.5×50mm	550	407	0.73	24
2		554	402	0.74	27
3		548	408	0.73	22
mean value		551	405	0.73	25
GB/T9711-2017		460~760	360~530	≤0.93	≥18

Table 7 Bending test results

Item/test specimen	Dimensions of test pieces	Span (mm)	Bending strength (MPa)
1	150×15mm	60	1178
2	150×15mm	60	1146
3	150×15mm	60	1142
4	150×15mm	60	1218

are weld height of 0–2mm, and local not more than 3mm and length not more than 50mm, the amount of misalignment is not more than $0.1T$ (T is the thickness of the thinner position at the butt joint, that is, 0.684mm). The inspection results found that the misalignment met the standard requirements; the maximum value of the root weld height was 4.6mm, which was 53% higher than the standard value; and the average value of the root weld height was 3.03mm, which was 51.5% higher than the standard value because the weld height at the root weld position is significantly higher than the minimum standard requirements and there is a certain amount of misalignment, which may lead to more serious stress concentration at the weld position.

Non-destructive testing

X-ray inspection of the failed ring weld was performed using a radiographic flaw detector. A tube voltage/tube current of 180KV/5mA was selected, and the inspection was performed in a single-wall, single-image transmission mode at an exposure time of 1min. The entire weld is divided into 6 sectors according to 60°for inspection, and the total number of films taken is 6. Testing detected a large number of cracks extending to different degrees along the circumferential direction of the weld in the inner surface of each sector. The crack length of the entire circumference accumulated 397 mm, accounting for about 75% of the circumference length (527.8 mm). X-ray inspection results are shown in Table 3.

Chemical analysis

The chemical composition of the base metal was tested by direct reading spectrometer according to the standard ASTM A751-14a. The results show that the base metal

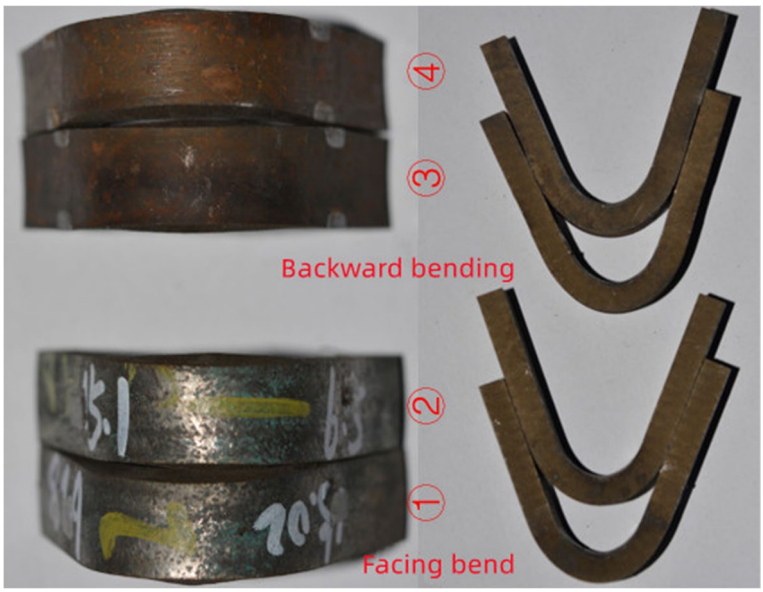

Fig. 3 Specimen after bend testing experiment

Table 8 Hardness test results

Sample	Test point hardness value (HV)								
A pipe section	152.9	154.1	154.9	154.1	151.9	154.1	154.6	160.1	159.2
B pipe section	154.6	154.6	159.3	163.5	155.9	162.8	148.3	155.6	157.9
Girth weld	201.2	215.5	198.6	193.7	183.9	185.7	194.7	199.3	208.3
SYT 0452-2012	≤250								

Table 9 Impact performance test results

Sample number	1	2	3	Mean value
Axial direction	31	27	31	30
Circumferential direction	30	29	30	30
Girth weld	25	26	25	25
SY/T 0452-2012	≥7 (J)			

meets the requirements of *GB/T9711-2017 steel pipe for pipeline transportation system of petroleum and natural gas industry*. The test data are shown in Table 4.

Mechanical properties analysis

Tensile test

Full-thickness tensile test of base metal of B pipe section The tensile test samples were prepared from the axial direction of the pipe. According to the standard *GB/T 228.1–2010 Tensile test of metal materials Part 1: Room temperature test method*, the tensile properties of the samples were evaluated by universal material testing machine. The

Table 10 Test results of weld samples without crack

Item	Weld microstructure	Fusion zone	Fine grain zone
No cracks Girth weld	Filling layer: IAF+GB+PF+P (Fig. 4) Root welding: PF+P (Fig. 5)	GB+PF+P (Fig. 6)	PF+P (Fig. 7)

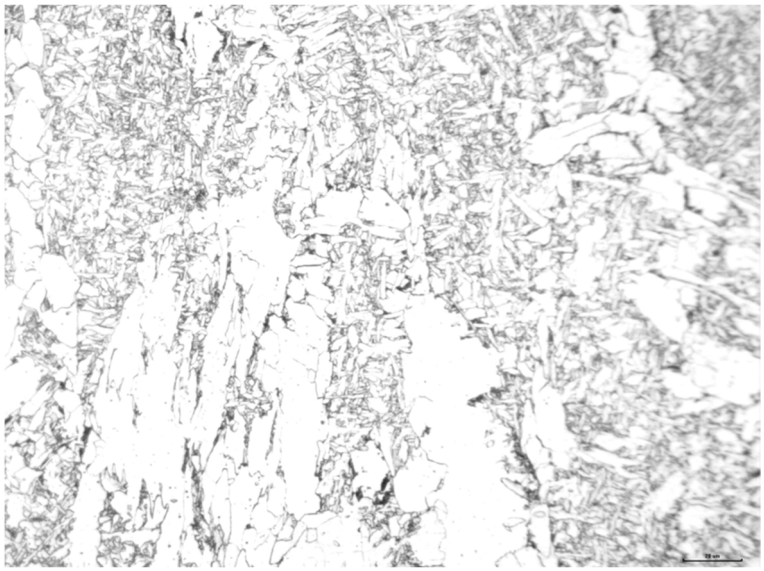

Fig. 4 Structure of filling layer of girth weld

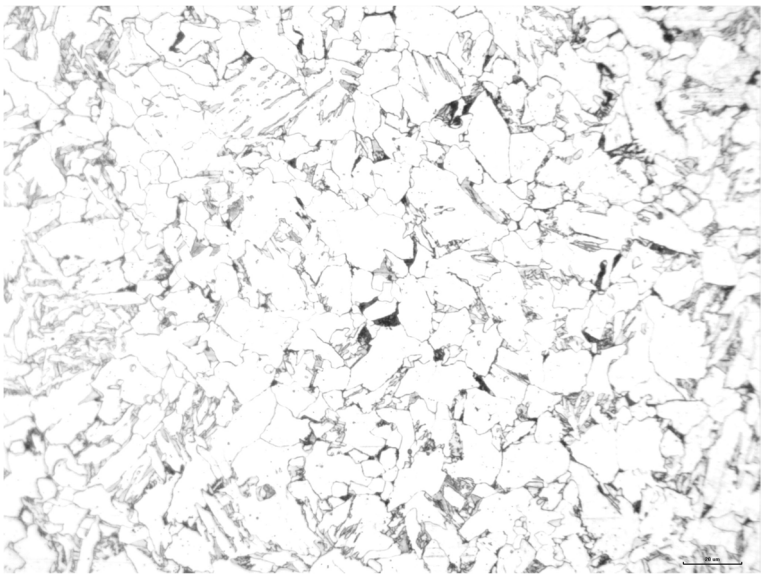

Fig. 5 Structure of root weld of girth weld

results show that the tensile properties of the pipe material meet the requirements of *GB/T9711-2017 steel pipe for pipeline transportation system of petroleum and natural gas industry*, as shown in Tables 4 and 5.

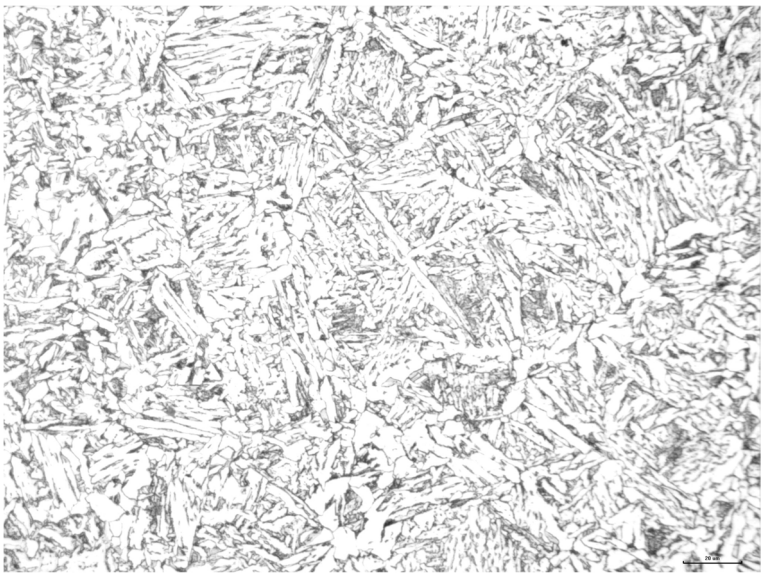

Fig. 6 Microstructure of fusion zone

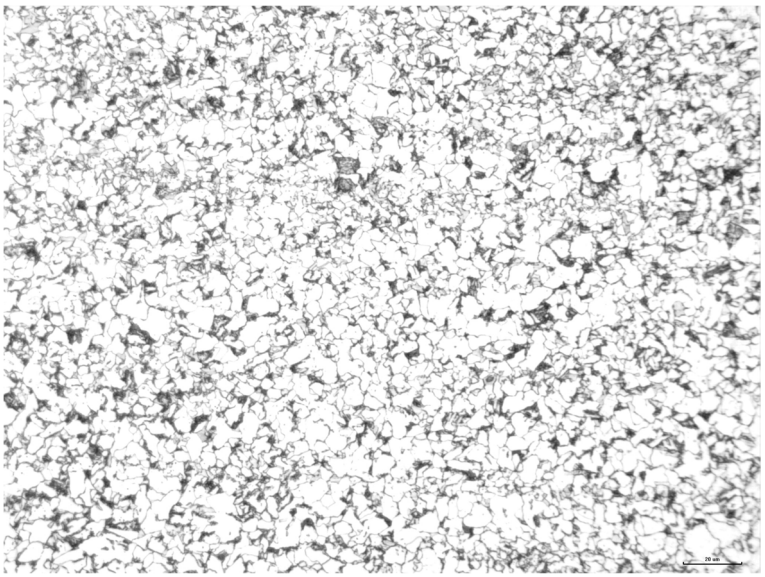

Fig. 7 Microstructure of fine-grained region

Full-thickness tensile test of weld The experimental specimens were intercepted at the location of the crack-free welds, and the results showed that the specimens met the requirements of the tensile properties standards. The data results are shown in Table 6.

Bending experiment

The full wall thickness bending test specimen was prepared from the axial direction of B pipe, and the universal material testing machine was used to carry out the experiment

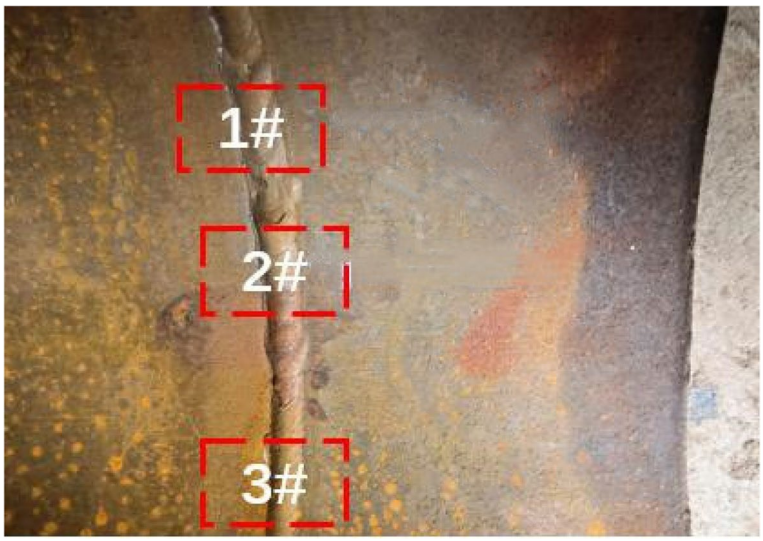

Fig. 8 Sampling position of cracked girth weld

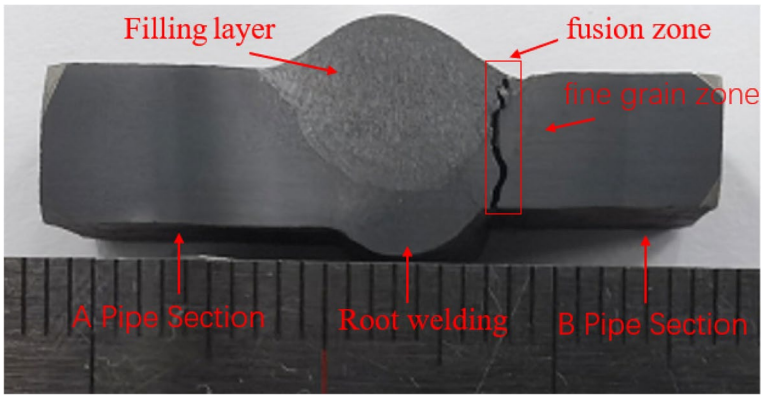

Fig. 9 Failure weld

Table 11 Test results of specimens at weld crack position

Item	Weld microstructure	Fusion zone	Fine grain zone
Invalid girth weld	Filling layer: IAF+GB+PF+P (Fig. 10) Root welding: PF+P (Fig. 11)	GB+PF+P (Fig. 12)	PF+P (Fig. 13)

according to the standard *GB / T232-2010 Metal material bending test method*. The experimental data are shown in Table 7. The standard *GB/T9711-2017 steel pipe for pipeline transportation system of petroleum and natural gas industry* stipulates that no crack should appear in any part of the sample after the bending test. The samples after the test were observed and analyzed. There were no cracks in any position of the experimental samples after the test, as shown in Fig. 3. The results show that the bending performance of the pipe meets the standard requirements.

Table 12 Test results of weld crack position

Item\number	Low magnification	High magnification
1#	The crack extended from the inner wall fusion zone and penetrated the entire wall thickness. The maximum crack width is about 0.4mm (Figs. 17, 18 and 19).	No welding defects such as inclusions, holes, or unfused metal were found around the crack, and no abnormal microstructure was found around the crack. There were many micro cracks along the crystal (Figs. 20, 21 and 22).
2#	The crack extended from the fusion zone of the inner wall, and there are extended cracks in the heat affected zone (Figs. 23 and 24).	No welding defects such as inclusions, holes, or unfused mental were found around the crack, and no abnormal microstructure was found around the crack. There were many microcracks along the crystal (Figs. 25 and 26).
3#	The crack extended from the fusion zone of the inner wall and is branched (Figs. 27 and 28).	No welding defects such as inclusions, holes, and unfused mental were found around the crack, and no abnormal microstructure was found around the crack. There were many microcracks along the crystal (Figs. 29, 30 and 31).

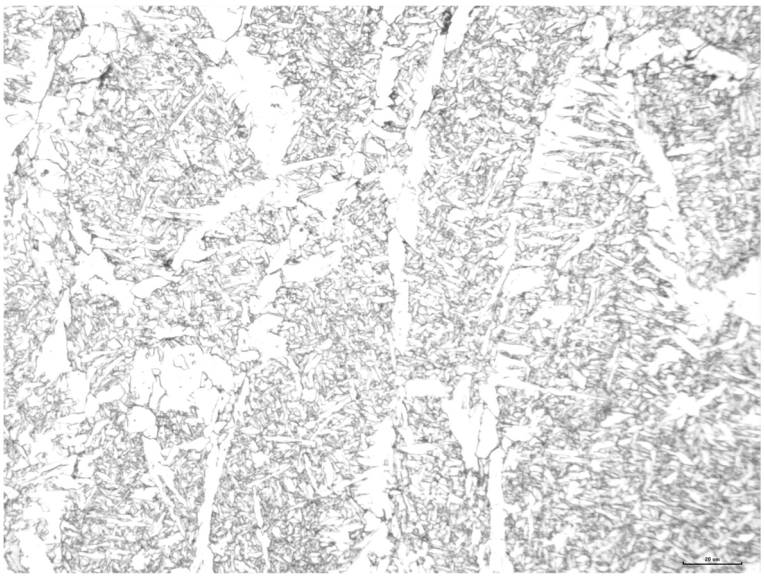

Fig. 10 Structure of filling layer of failed girth weld

Hardness experiment

According to the standard *GB/T 4340.1-2009 Vickers hardness test of metal materials Part 1: Test method*, the hardness test of base metal, weld, and heat affected zone of steel pipe was carried out by hardness tester. According to the requirements of *SY/T 0452-2012 oil and gas metal pipeline welding process evaluation*, the maximum allowable hardness of the base metal and weld of the steel pipe is 250 HV. The results show that the hardness test results of steel pipe base metal and girth weld meet the requirements. The test results are shown in Table 8.

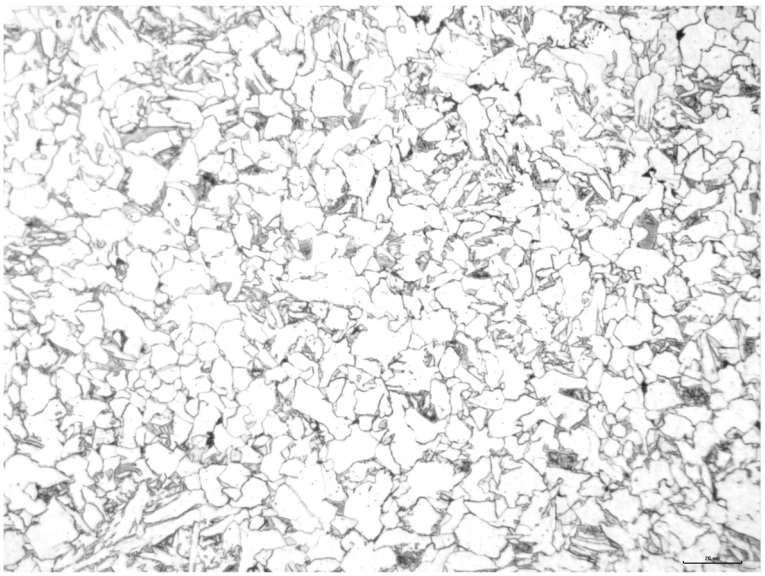

Fig. 11 Structure of root weld of failed girth weld

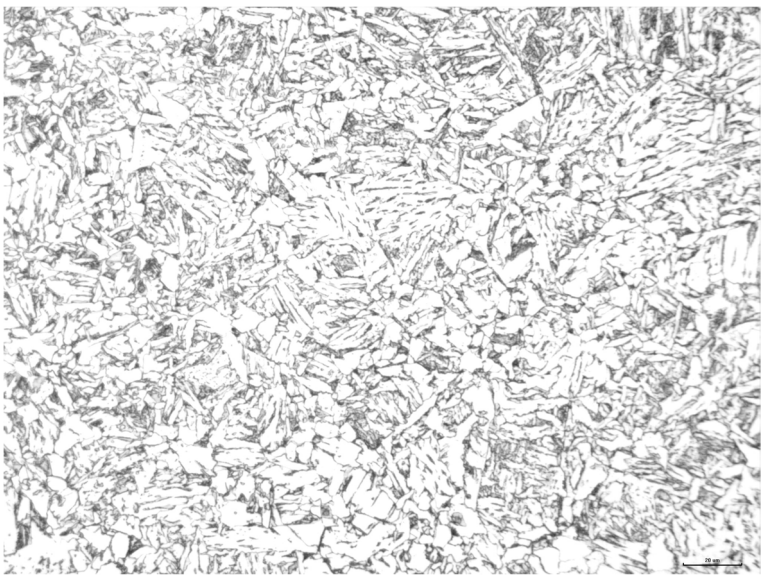

Fig. 12 Structure of fusion zone

Impact performance experiment

According to the standard *GB/T 229-2020 Charpy pendulum impact test method of metal materials*, Charpy impact test of base metal of steel pipe was carried out by impact testing machine. Three specimens were taken from the axial, circumferential, and circumferential weld positions of the B pipe to carry out impact tests. The *SYT 0452 - 2012 welding process evaluation of oil and gas metal pipelines* stipulates that the impact energy of 55mm×10 mm×2.5mm small sample should be greater than or equal to 7J. The results show that the impact energy of base metal and girth weld meet the standard requirements. The impact test data are shown in Table 9.

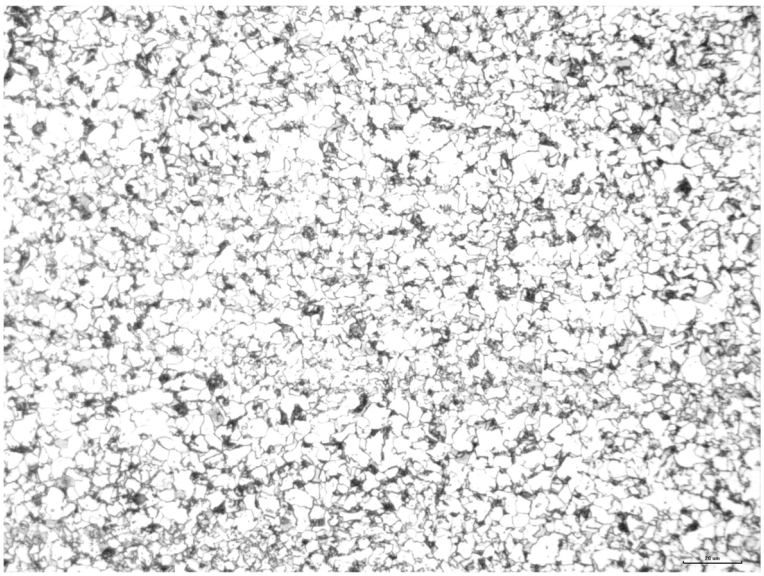

Fig. 13 Structure of fine-grained region

Table 13 Analysis results of microstructure of base metal

Item\number	Metallographic structure	Grain size	Inclusions
A pipe section	PF+P (Figs. 32 and 33)	11	D2.5
B pipe section	PF+P (Figs. 34 and 35)	11	D2.5

Metallographic analysis

Analysis of weld microstructure for weld without cracks

Two samples were taken from the weld without cracks for microstructure analysis. The analysis results are summarized in Table 10.

The girth weld metal of the metallographic specimen without crack is acicular ferrite + granular bainite + polygonal ferrite + pearlite structure (Fig. 4), the microstructure in the weld root is polygonal ferrite + pearlite (Fig. 5), the fusion zone structure is granular bainite + polygonal ferrite + pearlite structure (Fig. 6), and the structure in the fine grain zone is polygonal ferrite + pearlite (Fig. 7). No welding defects such as inclusions, holes, or unfused metal are found.

Microstructure analysis of weld cracking position

Three samples were taken at the cracking position of the girth weld to carry out metallographic analysis. The sampling positions are shown in Figs. 8 and 9, and the analysis results are summarized in Tables 11 and 12.

The microstructure of the filling layer of the cracked girth weld metallographic sample is acicular ferrite + granular bainite + polygonal ferrite + pearlite (Fig. 10), and the structure at the root of the weld is polygonal ferrite + pearlite (Fig. 11), the fusion zone structure is granular bainite + polygonal ferrite + pearlite (Fig. 12), the

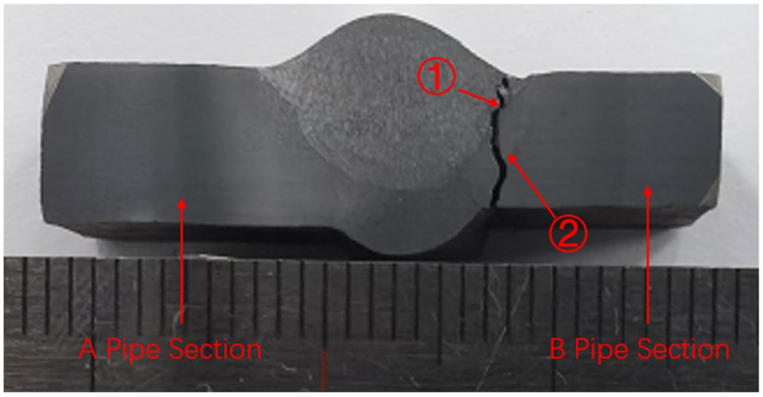

Fig. 14 Equivalent stress distribution at different weld heights

fine-grained zone structure is polygonal ferrite + pearlite structure (Fig. 13), and no abnormal structure is found.

Microstructure analysis of base metal

One specimen was taken from the A and B pipe sections near the cracking position of the failure girth weld for metallographic analysis. The results show that the base metal of the steel pipe is a multilateral ferrite structure, and the crack is located in the weld, close to the fusion boundary on the one side of the B pipe section. The microstructure of the weld near the crack is the same as that of the girth weld. The analysis results are summarized in Table 13.

CFD simulation

CFD method was used to further analyze the failure mechanism of the ring weld pipe. The analytical model of the failed pipe was established, and the fluid-structure coupling analysis was performed. Since there was no collapse or settlement of the ground, the external forces on the pipe were not considered. According to the data provided, the operating temperature of the pipe at the time of failure was 24.2°C and the actual average operating pressure of the pipe was 2.83 MPa. Considering these operating conditions, the load boundary conditions of the analytical model were set. Material parameters were obtained by actual material determination. Specifically, the yield strength and tensile strength of pipe section B were 395 MPa and 530 MPa, respectively; the yield strength and tensile strength of the weld were 405 MPa and 551 MPa, respectively; the Poisson's ratio was 0.3, and the modulus of elasticity was 200 GPa.

According to the steel pipe welding executive standard "*GB/T31032-2014 Welding and acceptance standard for steel pipings and pipelines*," the weld is set to have a smooth transition with the base metal, and the welding bevel is 65°. Under the condition that the girth weld has no misalignment, the cover weld height is 2mm, and the pipeline operating pressure is 2.83MPa; the root weld heights are set to 2mm, 3mm, 4mm, and 5mm, respectively; and the stress distribution of the welded joints is analyzed. As can be seen from Fig. 14, the greater the root weld height, the more severe the degree of stress concentration. The direction of fluid flow is from the B pipe to the A pipe, which also confirms from another perspective that the maximum stress-strain and cracks always appear at the weld near the side of pipe B.

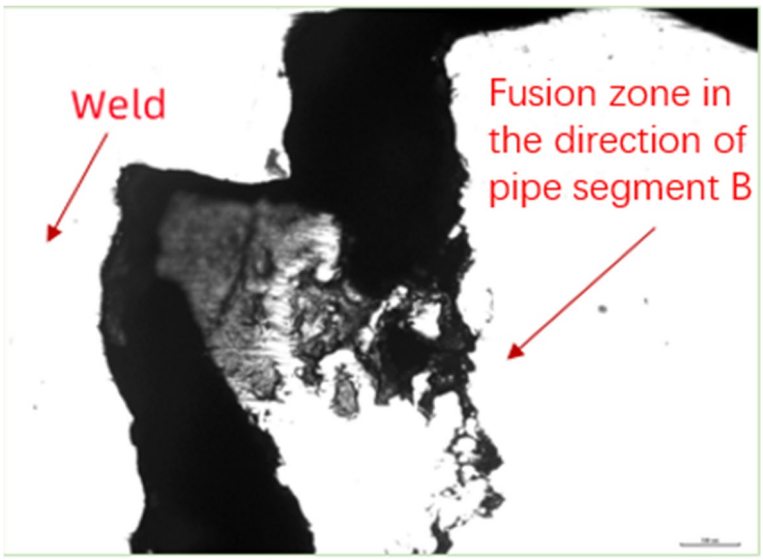

Fig. 15 Equivalent stress distribution of the weld at different weld heights

As shown in Fig. 15, by observing the stress distribution in the weld, the equivalent stress in the weld gradually increases from the outer region to the inner region and reaches a maximum value at the intersection of the bottom of the weld, where the crack damage occurs. According to the calculation results, although the maximum equivalent stress is not enough to directly cause cracking of the weld, the maximum equivalent force increases significantly with the increase of the root weld height under working conditions, and a relatively serious stress concentration occurs.

According to the data provided, since the pipeline has been put into operation for 2 months, the fluctuation range of the actual operating pressure is not very large, so the pressure fluctuation range is set to 1MPa in this analysis. Through the weld quality

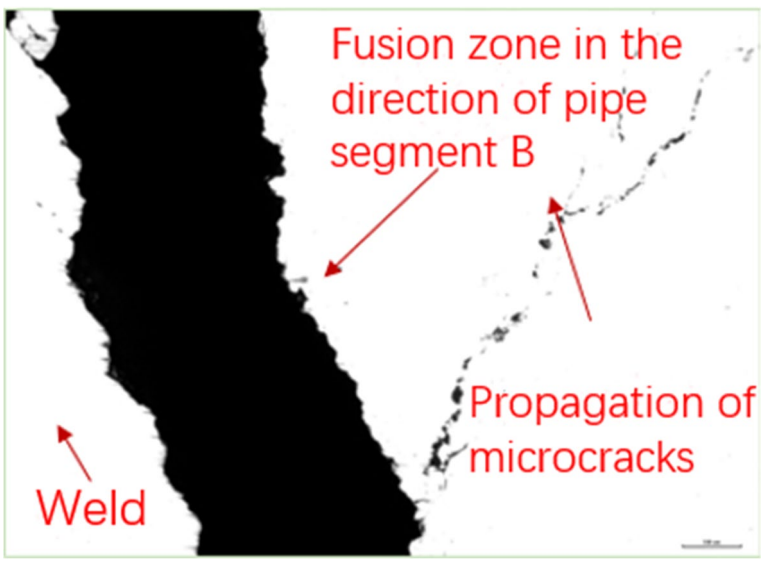

Fig. 16 Equivalent stress distribution under different operating pressure conditions

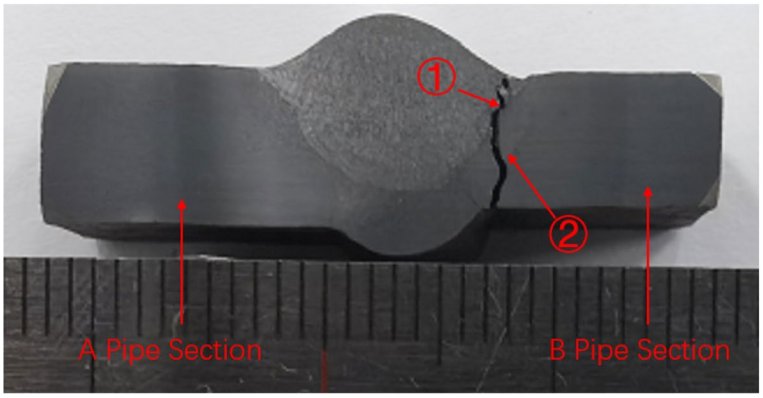

Fig. 17 Macro-morphology of 1# (the upper part is the outer surface)

inspection, the maximum root weld height of the ring weld pipe is 4.6 mm. In order to further analyze the impact of fluctuations in actual operating pressure on the welded joint, a pipe model with a root weld height of 4.6 mm was established, and the flow-solid coupling analysis was performed under the operating pressure conditions of 2.83 MPa, 3.33 MPa, and 3.83 MPa, respectively. As can be seen from Fig. 16, the operating pressure fluctuations have a significant impact on the stress of the welded joint, with the increase in operating pressure, the stress of the welded joint increases, and the degree of stress concentration becomes more and more serious. On the basis of the influence of the weld height, the formation of cracks will be accelerated.

Results

No obvious corrosion was found on the internal and external surfaces of the weld, and there was a tiny crack extending along the circumference of the weld on the external surface of the weld in the direction of the 12 o'clock position, with a crack length of

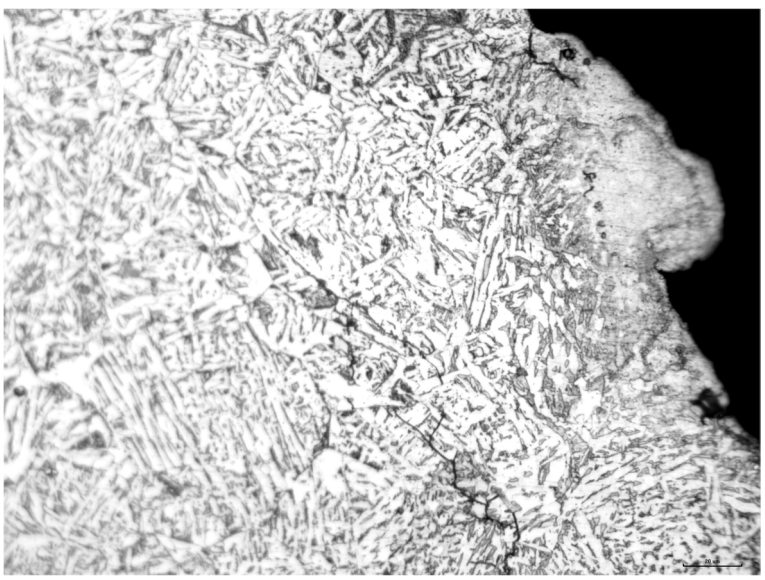

Fig. 18 Macro-morphology of 1# crack (position ① in Fig. 17)

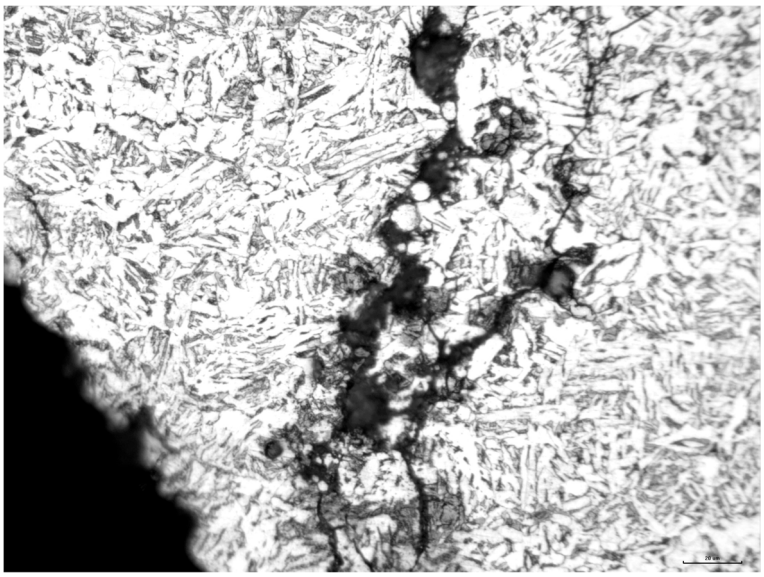

Fig. 19 Macro-morphology of 1# crack (position ② in Fig. 17)

about 40 mm, corresponding to a circumferential crack of about 140 mm in length and 0.46 mm in width on the internal surface of the weld. The crack was located on the base metal side of the B pipe section, immediately adjacent to the weld.

The X-ray inspection results of the pipe showed that there were a large number of cracks of different extension lengths along the circumference of the entire weld, all of which were located on the base metal side of the B section of the weld, immediately adjacent to the weld.

Through the analysis of the physical and chemical performance testing of the pipe, the tensile, impact, hardness, and other performance indicators of the base metal and the weld all meet the requirements of the standard "GB/T9711-2017 steel pipe for pipeline transportation system of petroleum and natural gas industry".

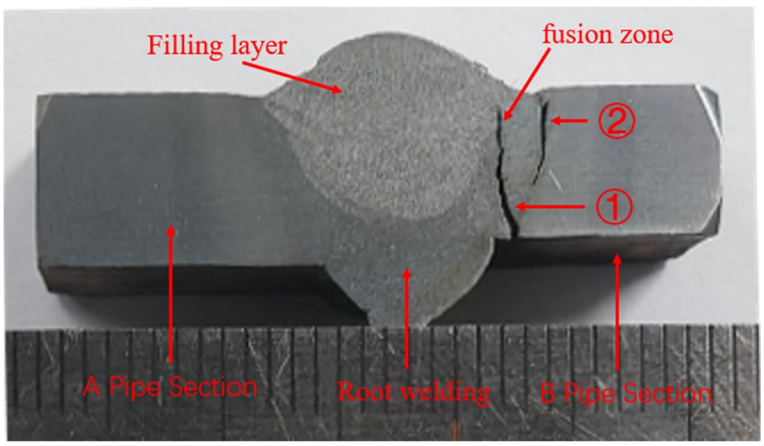

Fig. 20 Microstructure 1 at the crack of 1# (right side of position ① in Fig. 17)

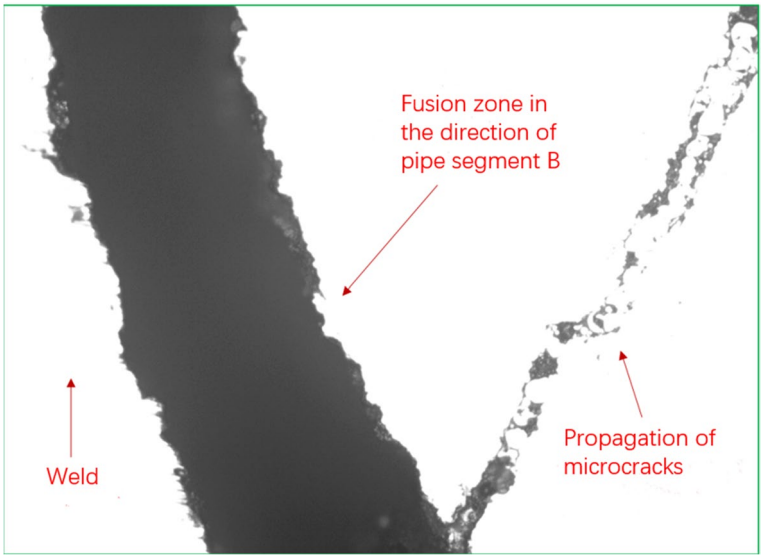

Fig. 21 Section 2 at the crack of 1# (left side of position ① in Fig.17)

By observing the metallurgical organization of the A pipe section, B pipe section base material, and the location of the crack in the ring weld; no abnormalities were found in the base material organization; and no welding defects such as inclusions, holes, and unfused welds were found in the weld metal.

According to the steel pipe welding executive standard "GB/T31032-2014 Welding and acceptance standard for steel pipings and pipelines," then combined with the weld quality inspection results found that the misalignment meets the standard requirements, the maximum value of the root weld height is 4.6mm, which is

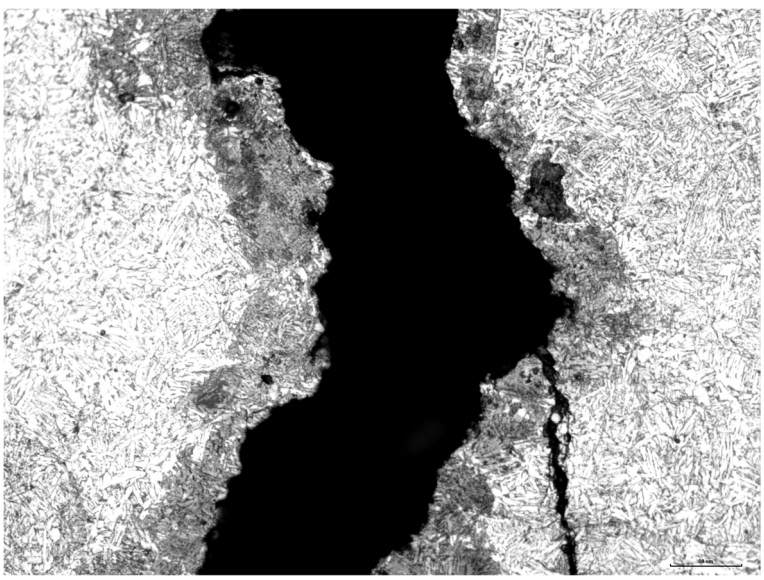

Fig. 22 Section 3 of the crack at 1# (position ② in Fig. 17)

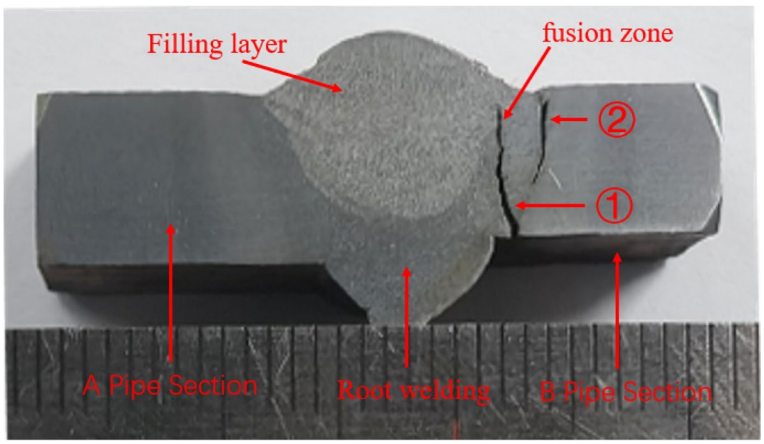

Fig. 23 Macroscopic appearance of 2# (the top is the outer surface)

53% higher than the standard value, and the average value of the root weld height is 3.03mm, which is 51.5% higher than the standard value.

According to the calculation results, the greater the root weld height, the more severe the degree of stress concentration. The operating pressure fluctuations also have a significant impact on the stress of the welded joint, with the increase in operating pressure, the stress of the welded joint increases, and the degree of stress concentration becomes more and more serious.

Discussion

Based on the non-destructive testing results of the weld and the macroscopic observation, it can be determined that the crack originated from the inner surface of the weld.

The cracks originated in the fusion zone on the side of the B pipe section, and there were a large number of microcracks along the crystal extending.

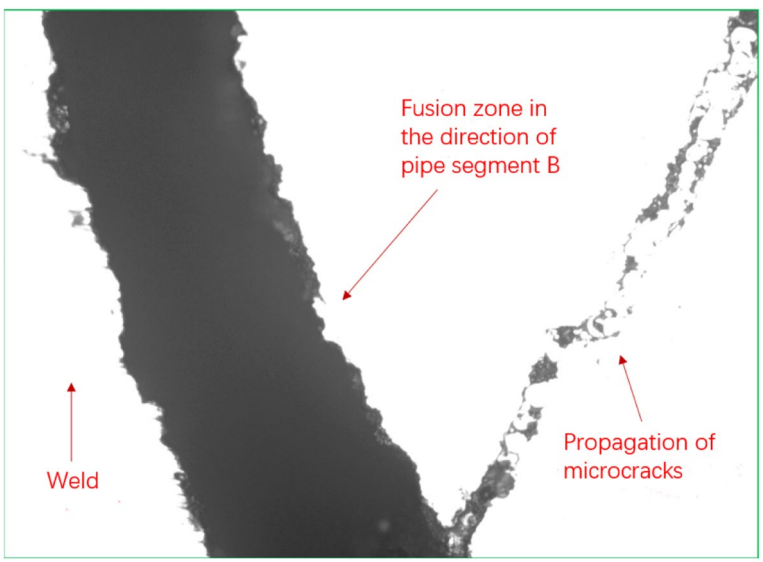

Fig. 24 Macroscopic appearance of 2# crack

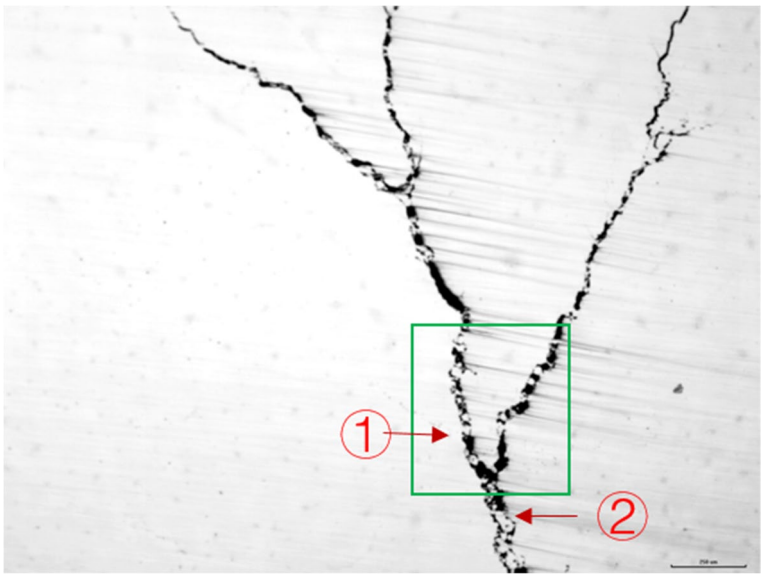

Fig. 25 Section 1 at the crack of 2# (position ① in Fig. 23)

The weld height at the root weld position is significantly higher than the minimum standard requirements, and there is a certain amount of misalignment, which may lead to more serious stress concentration at the weld position.

The fluid–solid coupling analysis shows that under working conditions, the weld height does not directly cause cracking of the pipe body and weld in the absence of defects in the pipe, but it causes severe stress concentration and has the effect of accelerating crack expansion.

Through a comprehensive analysis of the results of the experiment and CFD simulation, the cracking mode of the crack at the weld is the cracking along the crystal

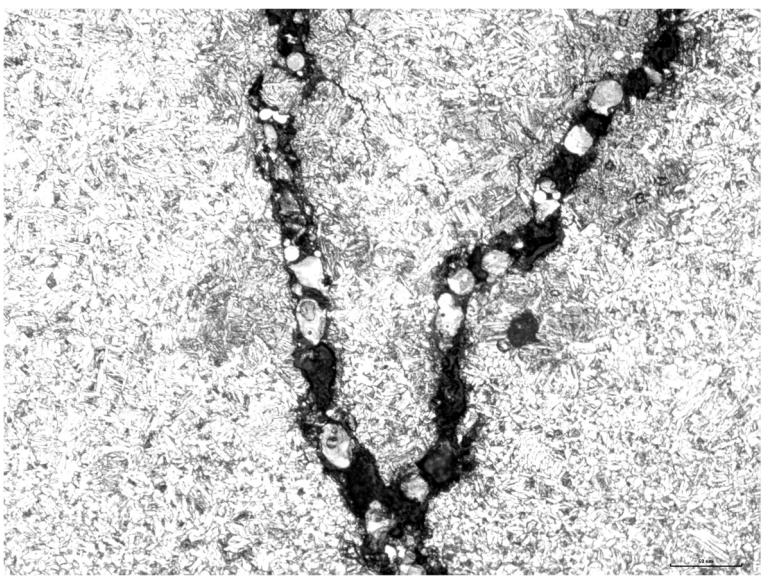

Fig. 26 Section 2 at the crack of 2# (position ② in Fig. 23)

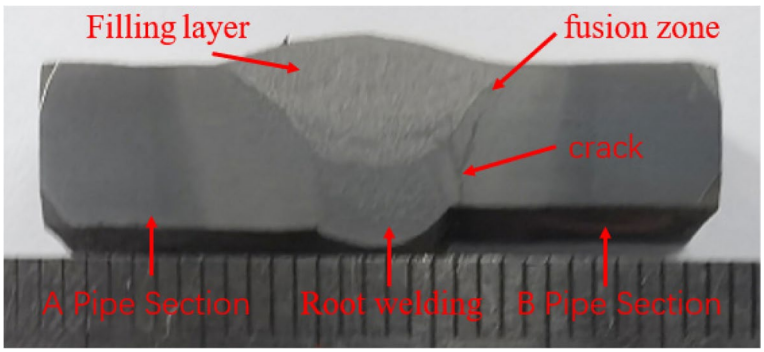

Fig. 27 Macroscopic appearance of 3# (the outer surface above)

under the internal stress of welding, and the possible reasons for the cracking are as follows. The stress concentration at the weld toe is mainly caused by the height of the weld, the greater the height of the weld, the more serious the degree of stress concentration, and the root weld position of the pipe is higher than the average height of 51.5% of the minimum standard requirements, resulting in the location of the weld is more severe stress concentration situation, which makes the weld inner surface of the fusion zone of the coarse crystal organization sprouting crack, and then continuously expand, and finally form cracks.

Several suggestions to prevent such a failure were proposed to avoid the occurrence of similar accidents. Improve tube manufacturing accuracy and reduce wall thickness variation, unequal wall thickness steel pipe should be thinned on the parts with large thickness before welding, and the welding process protocol should be strictly observed to improve the quality of the weld; preheat as much as possible before welding to reduce

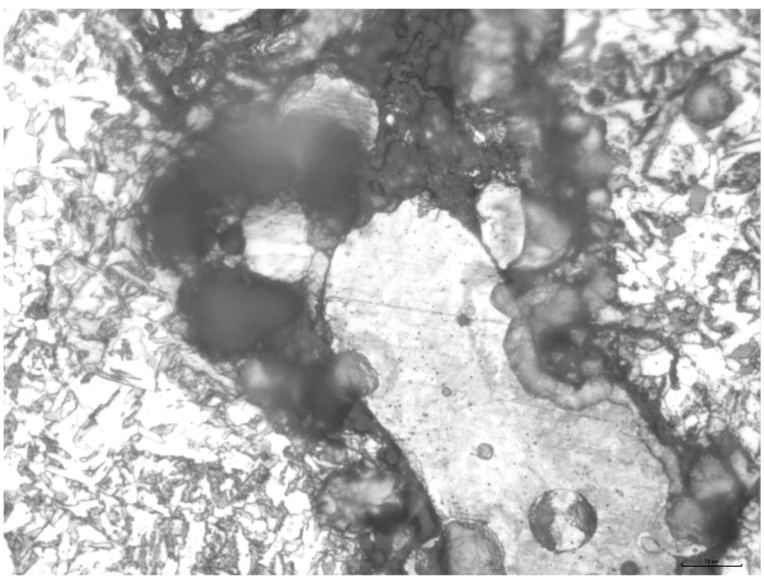

Fig. 28 Macroscopic appearance of 3# crack

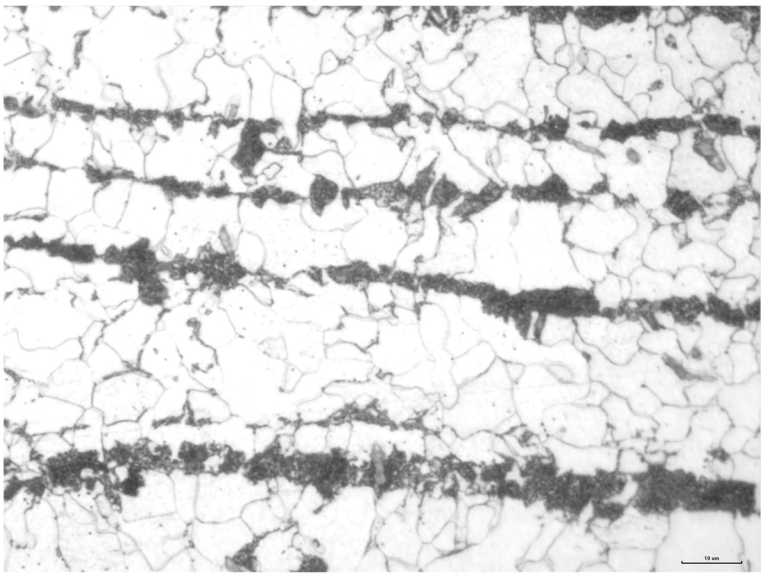

Fig. 29 Section 1 at the crack of 3# (the position of the green frame in Fig. 28)

the residual stress of welding and reduce the risk of cracking caused by stress concentration, and after welding is completed, try to eliminate the application of external forces to the weld that could lead to cracking of the weld.

Conclusions

Through the systematic detection, analysis, and simulation of the gas gathering pipeline welding cracking fault, the following conclusions are drawn:

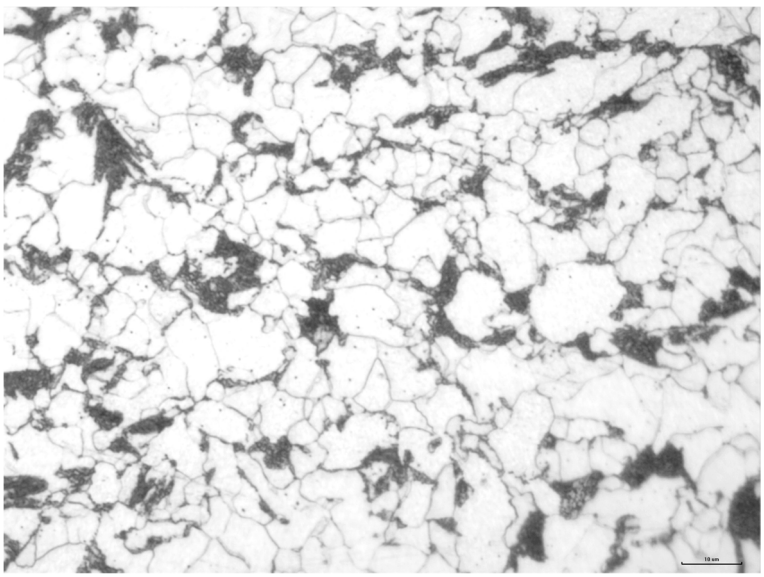

Fig. 30 Section 2 of the crack at 3# (position ① in Fig. 28)

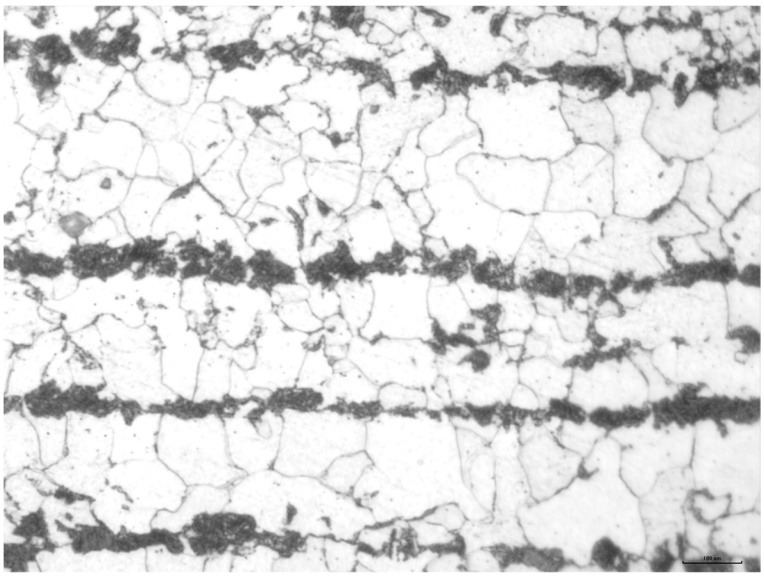

Fig. 31 Section 3 at the 3# crack (position ② in Fig. 28)

(1) The pipeline base metal meets the standard, and there are no welding defects such as inclusions, holes, and incomplete at the weld.
(2) The weld height is larger than the standard minimum requirement, resulting in more serious stress concentration at the weld position, and there is a certain amount of misalignment, which to a certain extent will aggravate the stress concentration caused by the height of the weld, thus making the fusion zone of the inner surface of the weld at the coarse crystal organization sprouts cracks, and then continuously extend, and eventually form cracks.

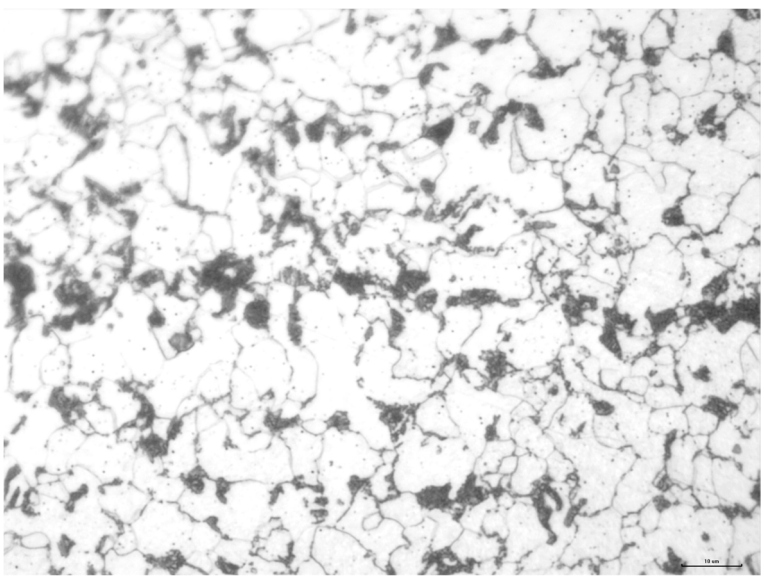

Fig. 32 A Pipe inner surface microstructure

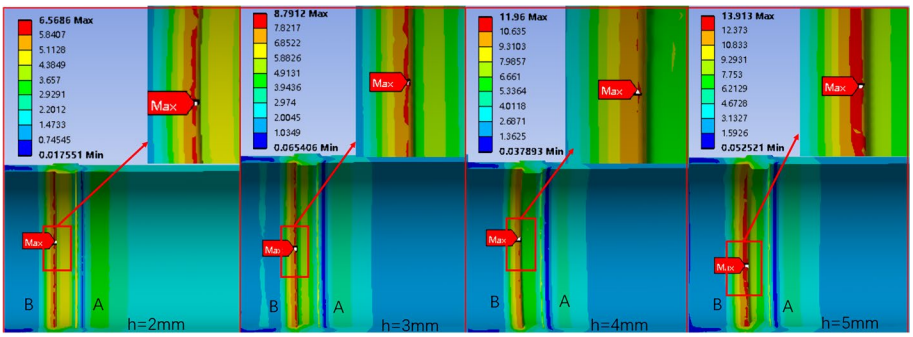

(a)

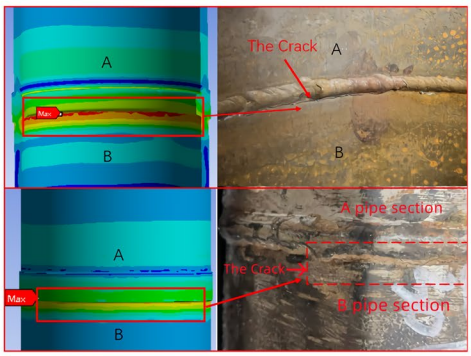

(b)

Fig. 33 A Pipe outer surface microstructure

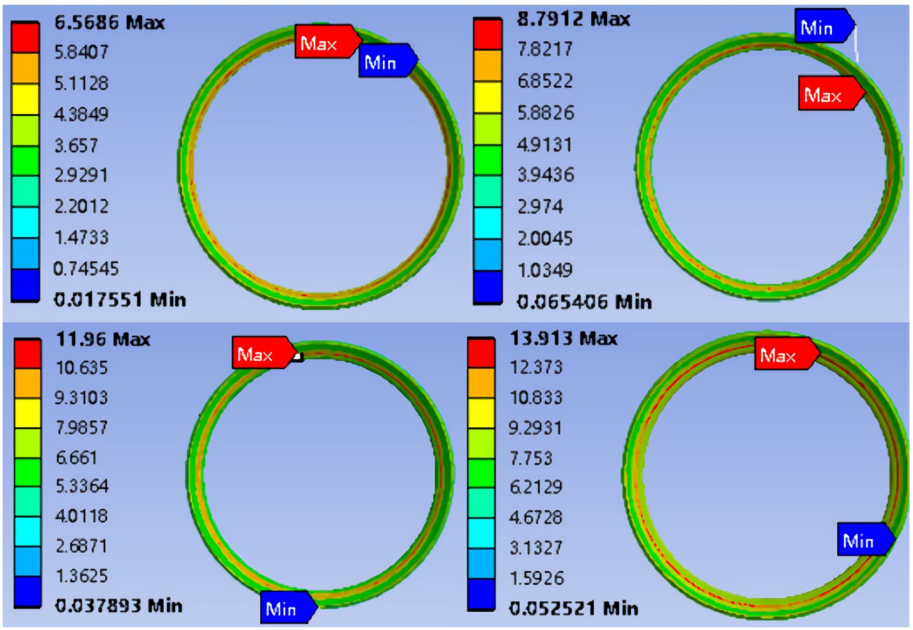

Fig. 34 B Pipe inner surface microstructure

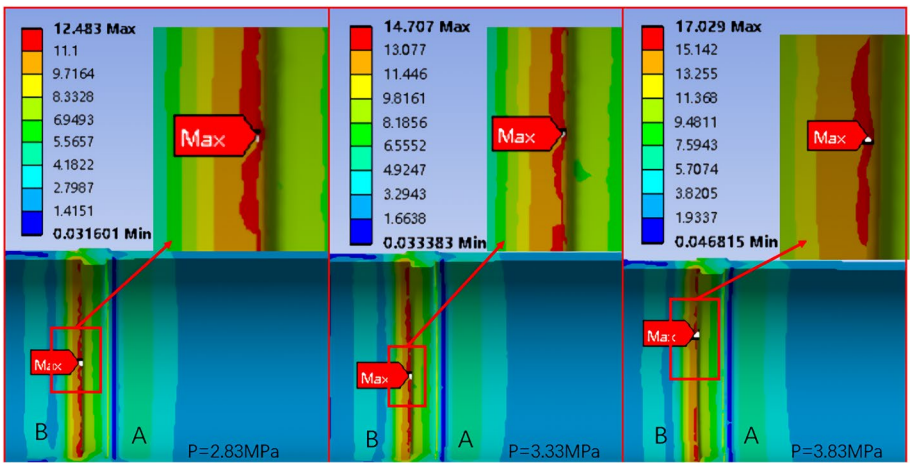

Fig. 35 B Pipe outer surface microstructure

(3) The cracking mode of the crack at the weld is the cracking along the crystal under the internal stress of welding.

(4) CFD simulation results show that although the stress concentration caused by the height of the weld does not directly lead to weld cracking, but under the influence of the stress concentration, cracks tend to sprout at the coarse grain organization of the fusion zone on the inner surface of the weld and can easily propagate throughout the weld and pipe wall thickness, leading to crack damage.

Abbreviations

IAF	Acicular ferrite
GB	Granular bainite
PF	Polygonal-like ferrite
P	Pearlite

Acknowledgements
Not applicable.

Authors' contributions
YC helped with the writing of the manuscript, provided the technical guidance, and was a major contributor in writing the manuscript. YX collected and analyzed the data and wrote the manuscript. JCL provided the ideas and guidance on the manuscript. WJW edited the manuscript and provided some references, and provided language modification and polishing for this article. The authors read and approved the manuscript.

Funding
Funded by the author.

Availability of data and materials
All materials and data used should be available at Southwest Petroleum University. The datasets used and/or analyzed during the current study are available from the corresponding author on reasonable request.

Declarations

Ethics approval and consent to participate
Not applicable.

Consent for publication
All the authors have agreed to publish this article.

Competing interests
The authors declare that they have no competing interests.

Received: 9 June 2022 Accepted: 2 August 2022
Published online: 22 October 2022

References

1. Luo Z, Yang Y (2021) Analysis and discussion on girth weld leakage failure of long distance natural gas pipeline. Welded Pipe Tube 44(11):33–39. https://doi.org/10.19291/j.cnki.1001-3938.2021.11.006
2. Yang F, Zhuo H, Luo J, Zhang L, Jia H (2015) Study of failure cause in some failure cases in oil and gas pipeline. Petroleum Tubular Goods Instruments 1(03):63–66. https://doi.org/10.19459/j.cnki.61-1500/te.2015.03.019
3. Kai X, Qiao G-y, Pan X-y, Chen X-w, Liao B, Xiao F-r (2020) Simulation of fatigue properties for the weld joint of the X80 weld pipe before and after removing the weld reinforcement. Int J Press Vessel Pip 187. https://doi.org/10.1016/j.ijpvp.2020.104164
4. Yunfeng H, Wang B, Yingchao X, Wang L, Cheng W (2020) Investigation on the fatigue crack propagation behavior of L360MS pipeline steel welded joints with Inconel 625 weld metal. Trans Indian Inst Metals 73. https://doi.org/10.1007/s12666-020-02041-4 prepublish
5. Sharma SK, Maheshwari S (2017) A review on welding of high strength oil and gas pipeline steels. J Nat Gas Sci Eng 38. https://doi.org/10.1016/j.jngse.2016.12.039
6. Bai F, Ding H, Tong L, Pan L (2020) Microstructure and properties of the interlayer heat-affected zone in X80 pipeline girth welds. Progress Nat Sci: Mater Int 30(1). https://doi.org/10.1016/j.pnsc.2019.08.010
7. Chirkov YA, Kushnarenko VM, Repyakh VS, Chirkov EY (2018) Analysis of the causes of failure of a pipeline welded joint. Metal Sci Heat Treatment 59(9). https://doi.org/10.1007/s11041-018-0209-2
8. Feng Q, Li R, Nie B, Liu S, Zhao L, Zhang H (2016) Literature review: theory and application of in-line inspection technologies for oil and gas pipeline girth weld defection. Sensors 17(1). https://doi.org/10.3390/s17010050
9. Gen LF, Quan F, Qing FA, Rui C (2021) Failure analysis for girth weld of gathering pipelines. Mater Sci Forum 6114. https://doi.org/10.4028/WWW.SCIENTIFIC.NET/MSF.1035.480
10. Jun C, Weifeng M, Guiliang P, Ke W, Junjie R, Hailiang N, Wei D, Tian Y (2021) Failure analysis on girth weld cracking of underground tee pipe. Int J Press Vessel Pip 191. https://doi.org/10.1016/J.IJPVP.2021.104371
11. Qiang L, Haoyu Y, Guo-chuan Z, Ke T, Peng-bo W, Sheng-yin S (2021) Investigation of weld cracking of a BOG booster pipeline in an LNG receiving station. Eng Fail Anal 122. https://doi.org/10.1016/J.ENGFAILANAL.2021.105247 prepublish
12. Shabani H, Goudarzi N, Shabani M (2018) Failure analysis of a natural gas pipeline. Eng Fail Anal 84. https://doi.org/10.1016/j.engfailanal.2017.11.003
13. Zhao Y, Song M (2016) Failure analysis of a natural gas pipeline. Eng Fail Anal 63. https://doi.org/10.1016/j.engfailanal.2016.02.023
14. Qiao Q, Cheng G, Wei W, Li Y, Huang H, Wei Z (2016) Failure analysis of corrosion at an inhomogeneous welded joint in a natural gas gathering pipeline considering the combined action of multiple factors. Eng Fail Anal 64. https://doi.org/10.1016/j.engfailanal.2016.02.015
15. Zhu L, Li J, Caihong L, Wei Z, Chen Z (2016) Leakage failure reason analysis of butt circumferential weld for a natural gas pipeline. Welded Pipe Tube 39(03):55–60. https://doi.org/10.19291/j.cnki.1001-3938.2016.03.012
16. Yuguang C, Qun C, Ying Z (2022) Numerical simulation of fracture behavior for the pipeline with girth weld under axial load. Engin Failure Anal. https://doi.org/10.1016/J.ENGFAILANAL.2022.106221 prepublish
17. Kai X et al (2020) Simulation of fatigue properties for the weld joint of the X80 weld pipe before and after removing the weld reinforcement. Int J Press Vessel Pip 187. https://doi.org/10.1016/j.ijpvp.2020.104164
18. Zhang M et al (2017) Effect of stress concentration on the fatigue strength of A7N01S-T5 welded joints. Int J Modern Phys B 31:16–19. https://doi.org/10.1142/S0217979217440477

Publisher's Note